Visualizing ^{13}C-labeled Metabolites in Maize Root Tips with Mass Spectrometry Imaging

Young Jin Lee*, Pubudu Nuwan Perera Hapuarachchige, Evan A. Larson, Ngoc Le, Trevor T. Forsman

Department of Chemistry

Iowa State University, Ames, IA, 50011, U.S.A.

* To whom correspondence should be addressed. E-mail: yjlee@iastate.edu

Keywords: *in vivo* isotope labeling, mass spectrometry imaging, MALDI, maize, root tip, ^{13}C-labeling

Abstract

Tracing *in vivo* isotope labeled metabolites has been used to study metabolic pathways or flux analysis. However, metabolic differences between the cells have been often ignored in these studies due to the limitation in solvent-based extraction. Here we demonstrate that the mass spectrometry imaging of *in vivo* isotope labeled metabolites, referred to as MSI*i*, can provide important insights into metabolic dynamics with cellular resolution that may supplement the traditional metabolomics and flux analysis. Developing maize root tips are adopted as a model system for MSI*i* by supplementing 200mM [U-^{13}C]glucose in 0.1x Hoagland medium. MSI*i* datasets were acquired for longitudinal sections of newly grown maize root tips after growing five days in the medium. A total of fifty-six metabolite features were determined to have been ^{13}C-labeled based on accurate mass and the number of carbon matching with the metabolite databases. Simple sugars and their derivatives were fully labeled but some small metabolites were partially labeled with a significant amount of fully unlabeled metabolites still present, suggesting the recycling of "old" metabolites in the newly grown tissues. Some distinct localizations were found, including the low abundance of hexose and its derivatives in meristem, the high abundance of amino acids in meristem, and the localization to epidermal and endodermal cells for lipids and their intermediates. Fatty acids and lipids were slow in metabolic turnover and showed various isotopologue distributions with intermediate building blocks, which may provide flux information in their biosynthesis.

Introduction

The use of stable isotope has been a powerful molecular biology tool since its discovery.[1] It is especially well suited when combined with modern mass spectrometry (MS) and now has become an essential strategy in large scale proteomics and metabolomics. *In vivo* stable isotope labeling has been shown to be an efficient method to identify unknown metabolites and discover new metabolic pathways.[2] It can be also used to measure metabolite flux such as ^{13}C-based metabolite flux analysis (13C-MFA) in central carbon metabolism.[3] In spite of their success, however, metabolomics and metabolite flux analysis mostly rely on solvent-based extraction of metabolites, which does not differentiate cells of different types.

Mass spectrometry imaging (MSI) has become a popular tool to visualize metabolites directly from tissue samples with single cell resolution.[4] It can simultaneously image tens or hundreds of metabolites without any labeling. There have been limited applications of *in vivo* stable isotope labeling for MSI. Nakabayashi et al. explored new nitrogen-containing metabolites in *Catharanthus roseus* with ^{15}N labeling and visualized their distributions in stem and root.[5] Dual isotope labeling of precursor metabolites was applied to Tyr and Phe metabolism in lemma and tomato fruits, and to reveal their spatially localized metabolites.[6] Romsdahl et al. visualized ^{13}C-labeled phosphatidylcholines in camelina and pennycress embryos by ^{13}C-labeling of developing siliques with [U-^{13}C]glucose.[7] Our group used ^{15}N-labeling of developing maize roots to visualize newly synthesized amino acids with external nitrogens.[8]

We envision that MSI with *in vivo* isotope labeling, here referred to as MSI*i*, can be a crucial tool to reveal metabolic dynamics with fine spatial details. Here we report its application to maize root tips with ^{13}C-labeling. Excised maize root tips can grow in a culture medium by supplementing glucose. This system has been used to study the oxygen uptake, energy charge, and

respiration of developing root tips under normoxia, anoxia, and/or hypoxia.[9] By using [U-^{13}C]glucose, Dieuaide-Noubhani et al. performed 13C-MFA of developing maize root tips and established pentose phosphate pathway (PPP) previously ignored in root tips.[10] Alonso et al. revealed the direct conversion of hexose-phosphate to glucose and substrate cycles in central metabolism under hypoxia.[11, 12] In this work, matrix-assisted laser desorption ionization (MALDI)-MSI has been performed to visualize various ^{13}C-labeled metabolites in developing maize root tips grown in a culture medium with [U-^{13}C]glucose, tentatively annotating 56 metabolites and revealing their localizations and metabolic turnover.

MATERIALS AND METHODS

Brief Experimental Details. Full details of the experimental section are given in the Supporting Information. The procedure for ^{13}C-labeling of maize root tips was based on Alonso et. al.[11] with some modifications. Briefly, maize root tips were cut at 3 mm length three days after the germination and grown in 0.1x Hoagland medium supplemented with 200 mM of [U-^{13}C] or unlabeled glucose for five days to the length of ~14 mm. The newly grown tissues were recut in 3 mm length from the tip and cryo-sectioned in longitudinal direction to acquire MS imaging data. MSI data were acquired using an Orbitrap mass spectrometer (QExactive HF; Thermo Fisher Scientific, San Jose, CA) coupled with a MALDI source (MALDI Injector; Spectroglyph, Kennewick, WA) at a resolution of 240,000 at *m/z* 200. Negative ion mode was used with 1,5-diaminonaphthaline (DAN) as a matrix and metabolites were detected as deprotonated, $[M-H]^-$, other than some adducts of highly abundant dihexose.

Results and Discussion

^{13}C-labeling of maize root tips and metabolite annotation

Maize root tips cut from the seeds can grow for multiple days in an inorganic salt medium supplemented with 200 mM glucose and continuous oxygen supply. It has been previously used for 13C-MFA using [U-^{13}C]glucose[10-12], which is adapted here to visualize ^{13}C-labeled metabolites in maize root tips. The root tip is composed of 1) root cap that protects the root as it grows, 2) meristem where cell division occurs, and 3) elongation zone where divided cells are elongated. As root cap is sometimes not clearly observed in MSI data, one can assume the very end of tip is mostly meristem (~0.3 mm in the main MSI data and ~1 mm in supporting MSI data) followed by the elongation zone. As the initial root tip (almost all ^{12}C) of ~3 mm length was grown to ~14 mm with ^{13}C supply before recutting at the length of ~3mm for MSI, ~20% of total biomass in the new tissue may still contain ^{12}C-materials from the original root tip, especially those metabolites with slow metabolic turnover. Two replicate MSI data sets obtained from the maize root tips grown in Petri dish and cryo-sectioned in longitudinal direction were used for metabolite annotations. Between the two, the one with the higher quality MS images was shown in this paper, which had overall in good agreement with the data set obtained from the cross-sectional tissue sections (not shown) and the data obtained with a different set up developed for a long-term growth (**Figures S1**).

Figure 1 compares the mass spectra of 12C and 13C data, MSI data of the control and ^{13}C-labeled, respectively, averaged over a portion of longitudinal tissue sections. Dihexose, most likely sucrose, was the base peak in both data but shifted by 12.040 Da in 13C data corresponding to the full ^{13}C-labeling of twelve carbons, +12ΔC where ΔC=^{13}C-^{12}C=1.00335 Da. Sucrose is readily synthesized from glucose in most plant cells including root tissues, and the same maize root tip system has been used by Alonso et al. to study the carbon flux of sucrose biosynthesis in maize

root tips.[13] Non-specific adducts of dihexose were also found due to its high concentration. Many peaks were matrix or other contaminations with no shift in peak positions, but some metabolites were detected with the peak shift corresponding to their number of carbons such as hexose phosphate, tripentose, and PI 34:2 shifted by +6ΔC, +15ΔC, and +43ΔC, respectively. Some cautions are necessary in the data interpretation such as the adducts of sucrose due to its high concentration.

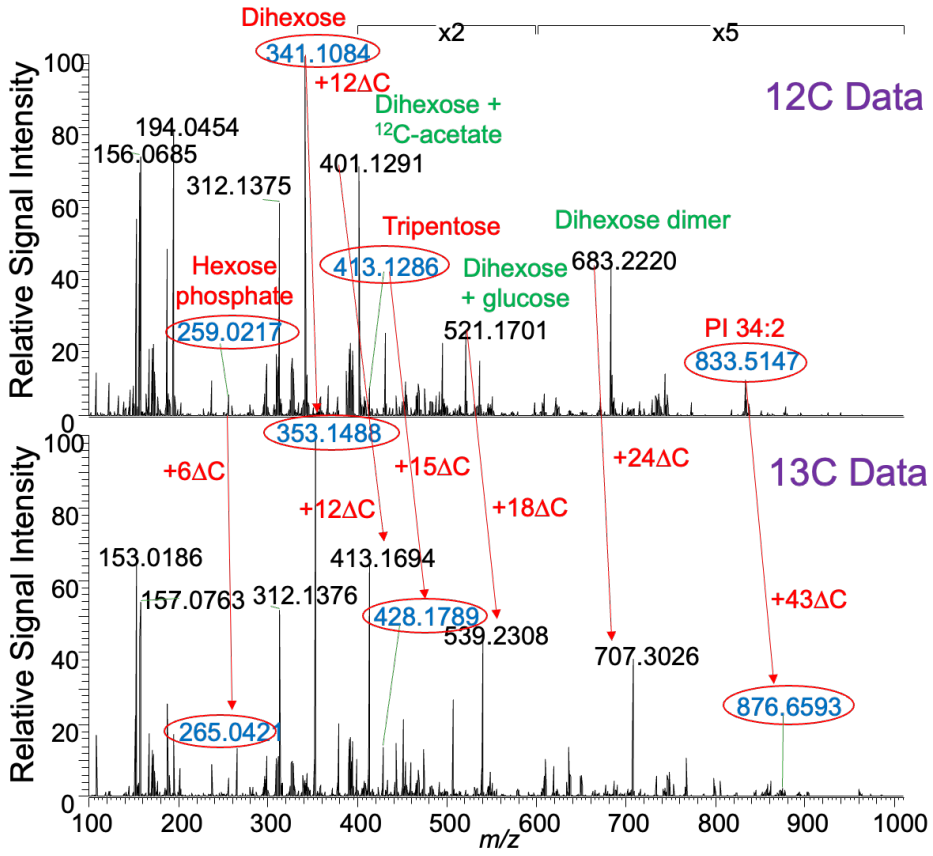

Figure 1. MALDI-MS spectra averaged over a portion of longitudinal tissue sections of maize root tips after grown 5 days in 0.1x Hoagland medium supplemented by **(top)** unlabeled glucose or **(bottom)** [U-^{13}C]glucose. Blue are the examples of true metabolites that are ^{13}C-labeled and shifted in 13C data corresponding to their number of carbons. Green are the adducts of dihexose

formed during MALDI process due to its high concentration including the adduct with ^{12}C-acetate contamination.

To systematically find ^{13}C-labeled metabolites, each MSI data set was averaged over the entire spectra and ^{13}C-labeled peaks in 13C data were matched to the corresponding monoisotopic peak in 12C data (called '12C peak' hereafter) within 2 ppm mass tolerance with an in-house Python code. For the metabolite features detected with at least two isotopologues in 13C data which may include monoisotopic peak (called 'M0 peak' hereafter to differentiate from 12C peak), annotation was made by searching 12C peaks against CornCyc/PlantCyc metabolite database (plantcyc.org) and METLIN metabolite database (metlin.scripps.edu). They were accepted as tentative identifications only if the theoretical mass was matching within 1 ppm mass tolerance after internal calibration and the carbon number was matching with the highest number of ^{13}C-labeling in 13C data (called '13C peak' hereafter). Multiple additional filtering was imposed to further improve the confidence: the MS images were localized to the tissue region for both 12C and 13C peaks, both 12C and 13C peaks had S/N above 10, and they were reproducibly found in another biological replicate with the same criteria. A total of fifty-six metabolites were tentatively annotated to have been ^{13}C-labeled as summarized in **Table S1**. These annotations were purely based on molecular formula and the compound names were arbitrarily chosen among the structural isomers except for some generic names (e.g., hexose) if deemed appropriate. About one thousand metabolite features were initially matched to have been ^{13}C-labeled by the program but more than 90% were excluded with the conservative filtering above. Primary metabolites were most represented in **Table S1** including amino acids, small organic acids, and sugars, but some lipids have been also detected.

Figure S1 shows an optical image of maize root tip with anatomical annotations. Active cell division occurs in meristem, protected by root cap as the root grows. Endodermis separates the inner vascular tissues from the outer cortex. **Figure 2a** shows selected MS images of simple sugars and their derivatives, comparing M0 peak ($^{12}C_n$) vs 13C peak ($^{13}C_n$) in 13C data, where n is the number of carbons in the molecule. These compounds were fully ^{13}C-labeled with no or very little M0 peak left in 13C data, which is not surprising as they are expected to be readily synthesized from glucose and almost no unlabeled $^{12}C_n$ compounds left in the newly grown tissues after five days. Similar behavior is also observed in other dimeric or trimeric sugars such as tripentose and methyl hexose dipentose (not shown). MS images showed relatively similar localization among these compounds. Essentially the same images were observed in a replicate (not shown) and another replicate obtained in a different setup designed for long-term growth (**Figure S2a**). For both **Figure 2a** and **Figure S2a**, hexose and deoxyhexose (red circle) had slightly less abundance at the very end of root tip, meristem, where active cell division occurs. There were hollow regions in all sugar images indicated by arrows, which may correspond to cryosectioned endodermis.

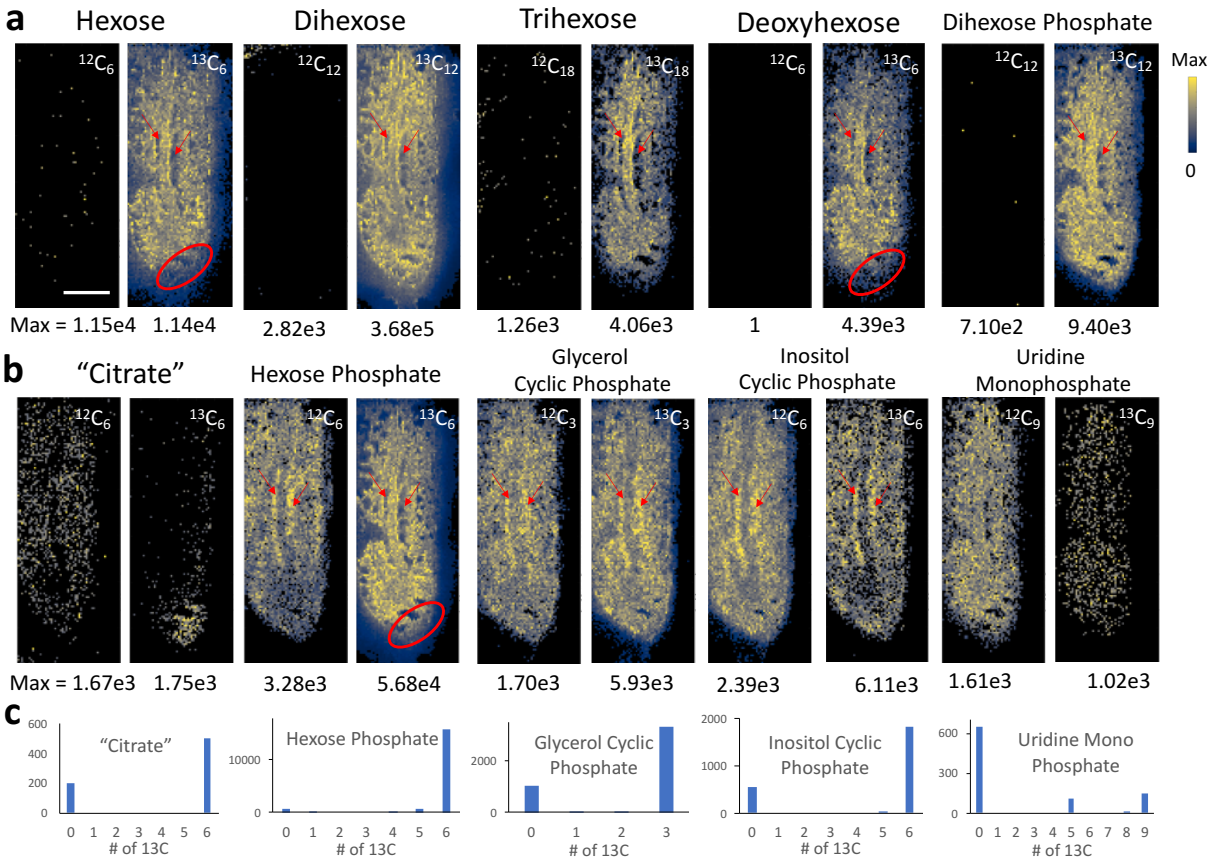

Figure 2. MS images of monoisotope ($^{12}C_n$) and fully labeled ($^{13}C_n$) compounds for **(a)** some sugars and their simple derivatives and **(b)** selected metabolites in 13C data of maize root tips labeled for 5 days. The scale bar is 0.5 mm. Circles and arrows indicate meristem region and endodermis, respectively. "Citrate" is a mixture of citrate and its structural isomer. **(c)** Isotopologue distributions of selected metabolites obtained from the average spectrum of the entire tissue, except for "citrate" which is from ROI of meristem region.

MS images and isotopologue distributions of some small metabolites

Unlike simple sugars shown in **Figure 2a**, most other metabolites showed a varying degree of M0 vs 13C peak intensities in their MS images as some examples shown in **Figure 2b**. 13C citrate was localized to the meristem, the same region circled in red for glucose and dihexose. Its

high abundance in meristem, but low abundance for glucose and sucrose, may indicate its active use in tricarboxylic acid (TCA) cycle. However, M0 "citrate" showed different image with 13C peak, suggesting it might be a structural isomer(s) that have a longer turnover time in old tissues. Uridine monophosphate (UMP) had higher M0 signal than 13C peak, while others have higher abundance for 13C peaks. The high abundance M0 signals composed of only ^{12}C atoms suggest the pre-existing unlabeled metabolites (i.e., $^{12}C_9$-UMP) were still widely available and utilized in the newly grown tissues even after five days in [U-$^{13}C_6$]glucose medium. Glycerol cyclic phosphate and inositol cyclic phosphate had high abundance regions in the middle of the tissue marked with arrows for both M0 and C13 peaks, which was in contrast to simple sugars and their derivatives in **Figure 2a** that had the hollow regions instead. Considering they have similar localization with fatty acids and lipids (see the later section), it may suggest they might be related with lipid metabolism and the arrow region is presumed to be endodermis.

13C peak of hexose phosphate showed similar localization with hexose; however, M0 peak showed completely different localization similar to glycerol cyclic phosphate and inositol cyclic phosphate. M0 and 13C peaks of hexose phosphate must be structural isomers with different localizations, dominated by unlabeled and ^{13}C-labeled, respectively. Unfortunately, the current study relies on accurate mass and cannot differentiate structural isomers. We hypothesize innositol-1-phosphate (I1P) is the major isomer for M0 peak and glucose-6-phosphate (G6P) and fructose-6-phosphate (F6P) for 13C peak. As intermediates for glycolysis, G6P and F6P would have a similar localization with glucose and almost completely have been ^{13}C-labeled, whereas I1P might have a slow turnover and a similar localization with lipids as an intermediate for the biosynthesis of phosphatidylinositol (PI)[14].

Figure 2c shows the isotopologue distributions of the metabolites shown in **Figure 2b**. They are uncorrected for natural ^{13}C isotope abundance or ^{12}C impurity in [U-^{13}C]glucose, but the contribution from natural ^{15}N or other stable isotopes are excluded thanks to ultrahigh mass resolution used in this study. Metabolic turnover rate can be calculated from the slope of the ^{13}C-fraction vs time curve.[15] In the assumption there is a gradual change from the ^{12}C-only metabolites to ^{13}C-only metabolites, overall metabolic turnover can be roughly estimated from 13C vs M0 ratio. The low abundance of 13C peak for UMP, 23% for 13C/M0 ratio, suggests their metabolic turnover was slow. In contrast, the high abundance of 13C peak in glycerol cyclic phosphate and inositol cyclic phosphate suggest they had relatively high metabolic turnover, although not as fast as simple sugars and their derivatives. Citrate also showed high turnover when the isotopologue distribution was obtained from the meristem region, but it cannot be used to estimate metabolite turnover rate as it may still contain some structural isomer in the region. UMP had interesting isotopologue distribution with distinct partial ^{13}C-labeling. UMP is composed of two carbon backbones, five-carbon pentose and four-carbon uridine. A significant amount of five ^{13}C-labeling, 18%, and no four ^{13}C-labeling suggests that pentose is readily synthesized from [U-$^{13}C_6$]glucose and the availability of uridine is the rate limiting step for the biosynthesis of UMP. Overall, similar results were obtained in biological replicates.

MS images and isotopologue distributions of amino acids

Ten amino acids were observed in **Table S1** including γ-amino butyric acid (GABA) and seven proteinogenic amino acids. **Figure 3a** shows the MS images of five abundant amino acids. GABA showed homogenous distributions, but proteinogenic amino acids were highly enriched in meristem near the root tips. Similar observation was made for Gln and Glu in the long-term growth

setup while it was not clear for other amino acids (**Figure S2c**). Interestingly, the relative isotope abundance between M0 and 13C peak was quite different among amino acids. The isotopologue distributions of amino acids are compared in **Figure 3b** with the simplified pathway of amino acid biosynthesis. Amino acids can be classified into five families depending on their intermediates where carbon skeletons are derived from in the central carbon metabolism[16]: serine family (Ser, Cys, Gly) from 3-phosphoglycerate, pyruvate family (Ala, Val, Leu) from pyruvate, aromatic family (Trp, Phe, Tyr) from 3-deoxy-arabinoheptulosonate-7-phosphate (DAHP), glutamate family (Glu, Gln, Pro, Arg, His, GABA) from α-ketogulutarate, and aspartate family (Asp, Asn, Met, Thr, Ile, Lys) from oxaloacetate. It should be noted that Leu and Ile have the same exact mass and cannot be distinguished.

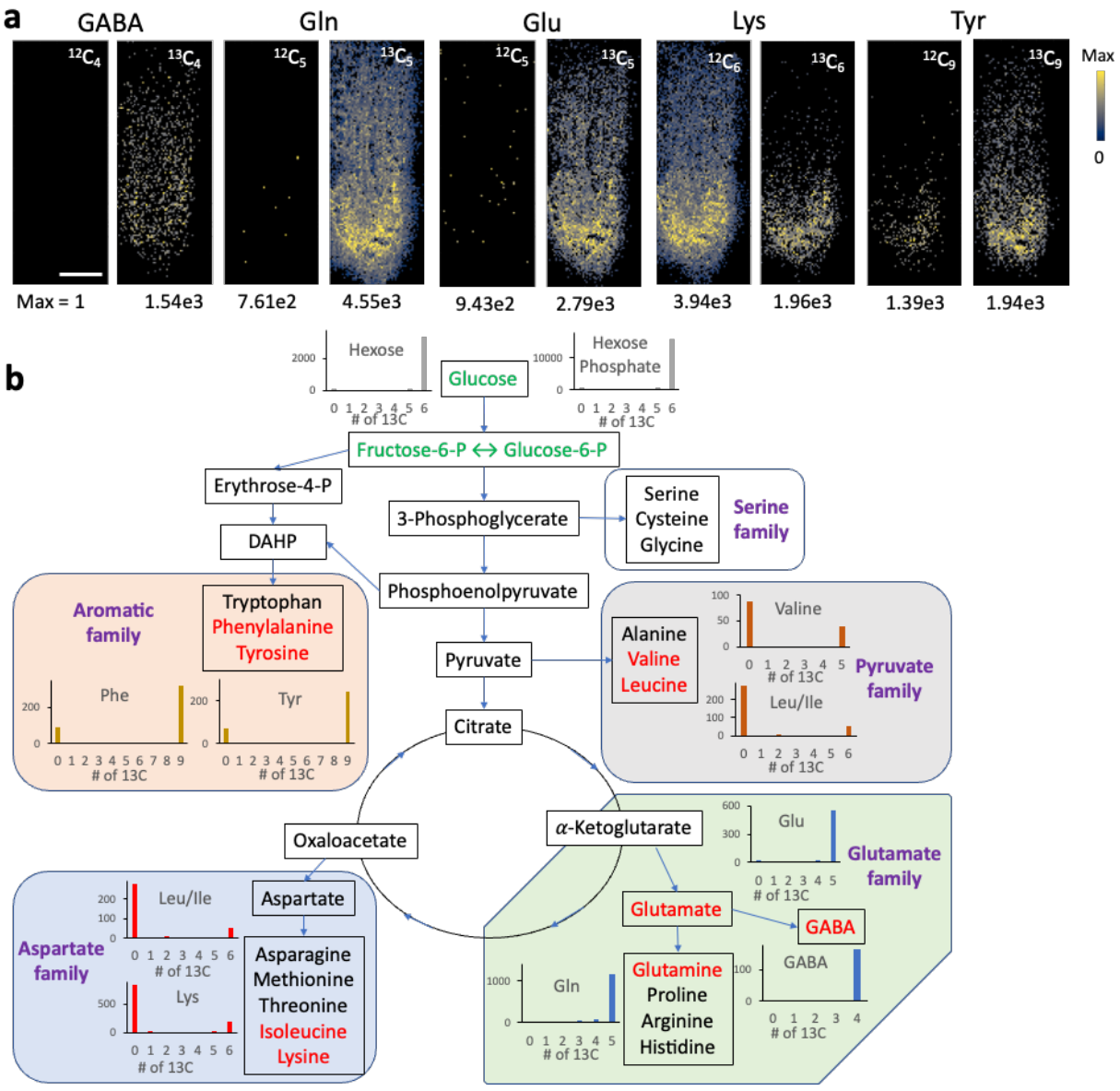

Figure 3. (a) MS images of selected amino acids in 13C data of maize root tips labeled for 5 days. The scale bar is 0.5 mm. **(b)** Isotopologue distributions of amino acids in the simplified biosynthesis pathway along the central carbon metabolism. Red font indicates detected amino acids.

None of serine family was detected most likely due to their low abundance, but at least two amino acids were detected in each of the other families. Interestingly, the relative isotope

abundance had the similar pattern within the family. Both the detected aromatic family members (Phe, Tyr) had ~3.5 times higher abundance for 13C peak compared to M0 whereas all three detected glutamate family members (Glu, Gln, GABA) were almost fully ^{13}C-labeled. In contrast, pyruvate and aspartate families had much higher M0 peak than 13C peaks. M0 abundance is the highest for Lys, about 4.5 times of 13C peak, and the lowest for Val, about twice. As a mixture, Leu/Ile had the relative isotope abundance between Val and Lys, but more similar to that of Lys. Similar observation was made in the biological replicate (not shown) and the replicate obtained in the long-term growth setup (**Figure S2c**). Considering central carbon metabolism have a fast turnover dominated by ^{13}C-labeled metabolites, the highly abundant M0 peaks in pyruvate and aspartate families suggest their metabolic turnover was slow. Fast turnover of glutamate family might be due to the high demand of Glu and Gln in many metabolic pathways (e.g., amino acid biosynthesis) and the relatively fast turnover of aromatic family might be due to its high demand for lignin biosynthesis.

MS images and isotope abundances of lipids

Lipids are another class of metabolites that were most detected in this study; three fatty acids, three cyclic phosphatidic acids (CPA), three lysophosphatidic acids (LPA), two lysophosphatidylinositols (LPI), two phosphatidic acids (PA) and one phosphatidylinositol (PI). **Figure 4** shows the representative MS images of selected lipids and their isotopologue distributions. Linoleic acid had a higher M0 abundance than 13C peak, suggesting the turnover of fatty acids was slow and unlabeled $^{12}C_n$ fatty acids were continuously being recycled in high abundance. The same trend was found for palmitic and oleic acids (not shown). The highly abundant region indicated by arrows is most likely endodermal cells, which was also detected in

many lipids (e.g., PI 34:2, PA 34:2) and lipid-related compounds (e.g., glycerol cyclic phosphate, inositol cyclic phosphate in **Figure 2b**). Unlike linoleic acids, PI 34:2 and PA 34:2 had almost no M0 peak and were present throughout the tissues but particularly at epidermal and endodermal cells, suggesting the membrane lipids of new tissues had at least partial ^{13}C-labeling. Similar observation was made in a replicate obtained in the long-term growth setup although not as clear due to low signals (**Figure S2d**).

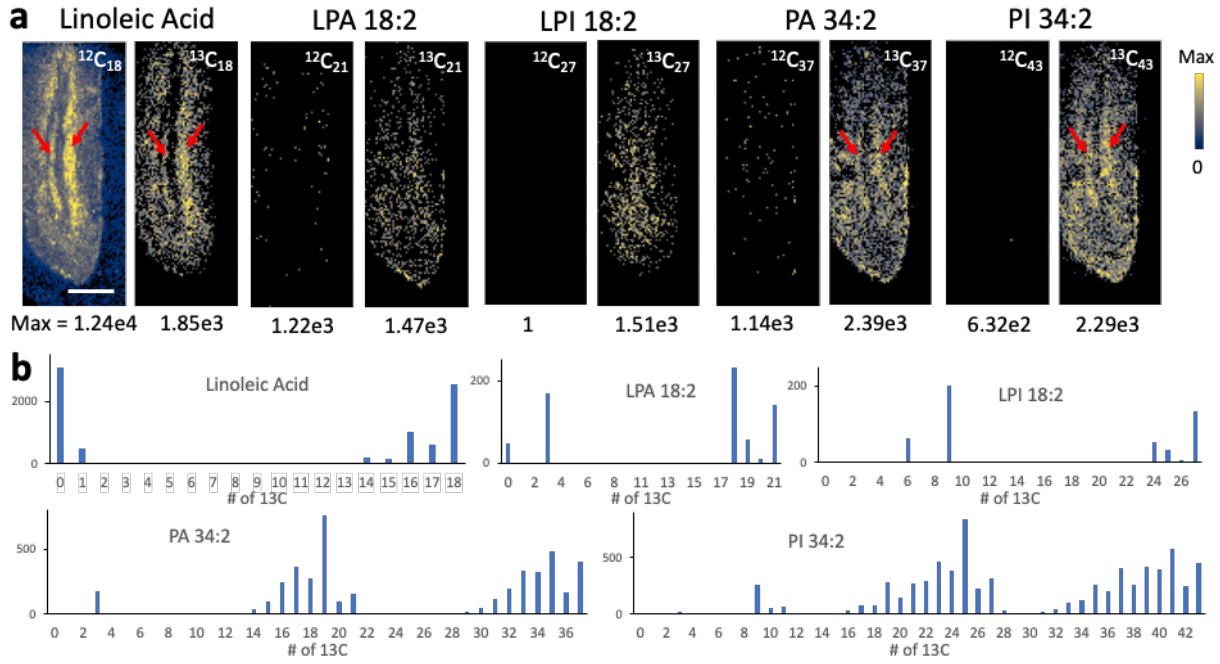

Figure 4. (a) MS images and **(b)** isotopologue distributions of linoleic acid and its lipids in 13C data of maize root tips labeled for 5 days. Arrows indicate endodermis. The scale bar is 0.5 mm.

The isotopologue distribution of lipids in **Figure 3b** showed an interesting intermediate behavior as seen in UMP. Partial ^{13}C-labeling of structural moieties has been reported in fatty acids and lipids, which was attributed to a large pool of acetyl Co-A or intact fatty acids.[17] M16 in linoleic acid had a high abundance although less than 13C peak (M18). Considering fatty acid biosynthesis occurs by adding two carbons at a time with acetyl-CoA, it might be an intermediate

that had been captured. As M16 linoleic acid has $^{13}C_{16}$ and $^{12}C_2$, it means the other two carbons were from $^{12}C_2$ acetyl-CoA, suggesting a plenty of unlabeled $^{12}C_2$ acetyl-CoA was available in new tissues even after growing in [U-^{13}C]glucose for five days. Similar intermediates can be seen in other lipids; e.g., highly abundant M35 and M41 in PA 34:2 and PI 34:2, respectively. Distinct abundance for M3 peak can be seen in PA 34:2 and LPA 18:2, which must have been originated from the rapidly synthesized glycerol backbone ($^{13}C_3$) with unlabeled $^{12}C_n$ fatty acyl chains. Similarly, distinct abundance of M9 peak can be seen in PI 34:2 and LPI 18:2, originated from the fast turnover of the glycerophosphate inositol backbone ($^{13}C_9$). Some combination of phospholipid backbone and one of the fatty acyl chains also showed distinctly high abundance of the intermediate ^{13}C-labeling. For example, M19 had the highest abundance in PA 34:2, corresponding to $^{13}C_3$-glycerol backbone and $^{13}C_{16}$-fatty acid (FA) 16:0 or 16:1, while the other fatty acyl chain must be $^{12}C_{18}$-FA 18:2 or 18:1. Similarly, the highest isotopologue abundance of M25 in PI 34:2 is attributed to the combination of $^{13}C_3$-glycerol backbone, $^{13}C_6$-inositol and $^{13}C_{16}$-FA16:0 or 16:1 with the other fatty acyl chain as $^{12}C_{18}$-FA 18:2 or 18:1. By carefully analyzing the isotopologue pattern of each lipid, it might be possible to estimate metabolic flux in lipid biosynthesis with high spatial resolution.

Limitation of this study

A technical advance made in this work may lead to metabolite flux imaging in the future; however, currently there are many limitations. One major limitation is the inability to resolve structural isomers as they will be detected at identical *m/z* even with ultrahigh mass resolution. This is a common challenge in mass spectrometry and typically requires separation such as GC or LC prior to MS. Unfortunately, separation techniques are often not compatible with MSI data

acquisition. Liquid microjunction surface sampling of each small pixel area coupled with LC-MS could be performed by sacrificing the spatial resolution to ~1 mm.[18] MS/MS imaging can be performed to determine the identity and localization of structural isomers,[19] while sacrificing throughput and the detection of other ions. Ion mobility spectrometry (IMS) can perform gas phase ion separation in millisecond time frame and can be combined with MALDI-MSI without scarifying spatial resolution.[20] However, time-of-flight mass spectrometers used in IMS-MS have the limited mass resolution of ~40,000, insufficient to distinguish most isotope fine structures. A combination of ultrahigh mass resolution MSI and IMS-MSI might be able to overcome this issue.

Another significant limitation of the current work is quantification. It is notoriously difficult to achieve absolute quantification in MSI due to ionization efficiency difference between analytes and ion suppression during ionization (or matrix effect)[21]. To address this issue, several methods have been developed including isotopically labeled internal standard[22] and mimetic tissue model with spiked internal standard[22]; however, they can typically quantify only one compound at a time. On the other hand, relative quantification among isotopologues is very reliable, as they have the same ionization efficiencies, and could be potentially used for carbon flux analysis of each intermediate metabolite. Even after solving all the technical issues, the two-dimensional nature of MSI cannot quantitatively represent flux in three-dimensional space.

Described above are general limitations of MSI, which becomes even more significant when one tries to derive spatially resolved flux analysis and biological conclusions from MSI*i*. Other limitations specific to MSI*i* include the chemical complexity and diluted isotopomer signals induced by isotope labeling. A lack of adequate software tools is another limitation. IsoScope can effectively visualize isotope-labeled metabolites, but is designed for pre-defined target compounds.[23] METASPACE, a web-based tool to annotate metabolites for MSI data, cannot

annotate isotope-labeled compounds.[24] Although not used in the current study due to the extensive internal calibration needed, it would be possible to annotate 12C data with METASPACE followed by IsoScope analysis for the annotated metabolites.

Conclusion

Largely relying on ultrahigh mass resolution, we have successfully demonstrated that ^{13}C-labeled metabolites can be traced and imaged using MALDI-MSI for the maize root tip system. Some metabolites showed differences in localization and metabolic turnover, suggesting potential flux imaging in the future. Particularly, the high abundance of certain building blocks in the isotopologue pattern of UMP and lipids suggests its potential usefulness to determine relative metabolic activities in biosynthesis. It is very unlikely flux imaging could be achieved anytime soon due to many limitations, especially quantification and differentiating structural isomers. However, we envision the MSI of *in vivo* isotope labeled metabolites demonstrated in this work could provide useful information for 13C-MFA. Some of the hypothesis made in 13C-MFA might be verified; for example, the cellular differences for a specific metabolism by extracting isotopologue patterns from specific cells or tissue locations. MSI*i* is currently in an exploratory stage, but combined with MFA, it could reveal dynamic nature of cell metabolism in unprecedented details.

Supporting Information

The Supporting Information is available free of charge on the ACS Publications website.

Supplementary methods, tentatively annotated labeled metabolites, optical image with anatomical description, selected MS images from long-term growth setup (pdf).

Data availability

MALD-MSI datasets are deposited in the Mass Spectrometry Interactive Virtual Environment (https://massive.ucsd.edu) with the accession number MSV000091017. The python program is available at Github: https://github.com/yjlee-ISU/label_finder

Acknowledgement

This work is supported by National Science Foundation under Grant No. 2150468.

References

(1) Lehmann, W. D. A timeline of stable isotopes and mass spectrometry in the life sciences. *Mass Spectrom. Rev.* **2017**, *36* (1), 58-85. DOI: https://doi.org/10.1002/mas.21497.
(2) Llufrio, E. M.; Cho, K.; Patti, G. J. Systems-level analysis of isotopic labeling in untargeted metabolomic data by X13CMS. *Nat. Protoc.* **2019**, *14* (7), 1970-1990. DOI: 10.1038/s41596-019-0167-1.
(3) Zamboni, N.; Fendt, S.-M.; Rühl, M.; Sauer, U. 13C-based metabolic flux analysis. *Nat. Protoc.* **2009**, *4* (6), 878-892. DOI: 10.1038/nprot.2009.58.
(4) Lee, Y. J.; Perdian, D. C.; Song, Z.; Yeung, E. S.; Nikolau, B. J. Use of mass spectrometry for imaging metabolites in plants. *Plant J.* **2012**, *70* (1), 81-95. DOI: 10.1111/j.1365-313X.2012.04899.x.
(5) Nakabayashi, R.; Hashimoto, K.; Toyooka, K.; Saito, K. Top-down Metabolomic Approaches for Nitrogen-Containing Metabolites. *Anal. Chem.* **2017**, *89* (5), 2698-2703. DOI: 10.1021/acs.analchem.6b04163. Nakabayashi, R.; Mori, T.; Takeda, N.; Toyooka, K.; Sudo, H.; Tsugawa, H.; Saito, K. Metabolomics with 15N Labeling for Characterizing Missing Monoterpene Indole Alkaloids in Plants. *Anal. Chem.* **2020**, *92* (8), 5670-5675. DOI: 10.1021/acs.analchem.9b03860.
(6) Feldberg, L.; Dong, Y.; Heinig, U.; Rogachev, I.; Aharoni, A. DLEMMA-MS-Imaging for Identification of Spatially Localized Metabolites and Metabolic Network Map Reconstruction. *Anal. Chem.* **2018**, *90* (17), 10231-10238. DOI: 10.1021/acs.analchem.8b01644.
(7) Romsdahl, T. B.; Kambhampati, S.; Koley, S.; Yadav, U. P.; Alonso, A. P.; Allen, D. K.; Chapman, K. D. Analyzing Mass Spectrometry Imaging Data of 13C-Labeled Phospholipids in Camelina sativa and Thlaspi arvense (Pennycress) Embryos. *Metabolites* **2021**, *11* (3), 148.
(8) O'Neill, K. C.; Lee, Y. J. Visualizing Genotypic and Developmental Differences of Free Amino Acids in Maize Roots With Mass Spectrometry Imaging. *Frontiers in Plant Science* **2020**, *11* (639), Original Research. DOI: 10.3389/fpls.2020.00639.

(9) Saglio, P. H.; Drew, M. C.; Pradet, A. METABOLIC ACCLIMATION TO ANOXIA INDUCED BY LOW (2-4 KPA PARTIAL-PRESSURE) OXYGEN PRETREATMENT (HYPOXIA) IN ROOT-TIPS OF ZEA-MAYS. *Plant Physiol.* **1988**, *86* (1), 61-66. DOI: 10.1104/pp.86.1.61. Saglio, P. H.; Raymond, P.; Pradet, A. METABOLIC-ACTIVITY AND ENERGY-CHARGE OF EXCISED MAIZE ROOT-TIPS UNDER ANOXIA - CONTROL BY SOLUBLE SUGARS. *Plant Physiol.* **1980**, *66* (6), 1053-1057. DOI: 10.1104/pp.66.6.1053. Saglio, P. H.; Pradet, A. SOLUBLE SUGARS, RESPIRATION, AND ENERGY-CHARGE DURING AGING OF EXCISED MAIZE ROOT-TIPS. *Plant Physiol.* **1980**, *66* (3), 516-519. DOI: 10.1104/pp.66.3.516. Brouquisse, R.; James, F.; Raymond, P.; Pradet, A. STUDY OF GLUCOSE STARVATION IN EXCISED MAIZE ROOT-TIPS. *Plant Physiol.* **1991**, *96* (2), 619-626. DOI: 10.1104/pp.96.2.619.
(10) Dieuaide-Noubhani, M.; Raffard, G.; Canioni, P.; Pradet, A.; Raymond, P. Quantification of compartmented metabolic fluxes in maize root tips using isotope distribution from 13C- or 14C-labeled glucose. *J. Biol. Chem.* **1995**, *270* (22), 13147-13159. DOI: 10.1074/jbc.270.22.13147 From NLM.
(11) Alonso, A. P.; Raymond, P.; Rolin, D.; Dieuaide-Noubhani, M. Substrate cycles in the central metabolism of maize root tips under hypoxia. *Phytochemistry* **2007**, *68* (16), 2222-2231. DOI: https://doi.org/10.1016/j.phytochem.2007.04.022.
(12) Alonso, A. P.; Vigeolas, H. l. n.; Raymond, P.; Rolin, D.; Dieuaide-Noubhani, M. A New Substrate Cycle in Plants. Evidence for a High Glucose-Phosphate-to-Glucose Turnover from in Vivo Steady-State and Pulse-Labeling Experiments with [13C]Glucose and [14C]Glucose. *Plant Physiol.* **2005**, *138* (4), 2220-2232. DOI: 10.1104/pp.105.062083 (acccessed 7/31/2021).
(13) Alonso, A. P.; Raymond, P.; Hernould, M.; Rondeau-Mouro, C.; de Graaf, A.; Chourey, P.; Lahaye, M.; Shachar-Hill, Y.; Rolin, D.; Dieuaide-Noubhani, M. A metabolic flux analysis to study the role of sucrose synthase in the regulation of the carbon partitioning in central metabolism in maize root tips. *Metab. Eng.* **2007**, *9* (5), 419-432. DOI: https://doi.org/10.1016/j.ymben.2007.06.002.
(14) Gardocki, M. E.; Jani, N.; Lopes, J. M. Phosphatidylinositol biosynthesis: Biochemistry and regulation. *Biochim. Biophys. Acta* **2005**, *1735* (2), 89-100. DOI: https://doi.org/10.1016/j.bbalip.2005.05.006.
(15) Hasunuma, T.; Harada, K.; Miyazawa, S.-I.; Kondo, A.; Fukusaki, E.; Miyake, C. Metabolic turnover analysis by a combination of in vivo13C-labelling from 13CO2 and metabolic profiling with CE-MS/MS reveals rate-limiting steps of the C3 photosynthetic pathway in Nicotiana tabacum leaves. *J. Exp. Bot.* **2010**, *61* (4), 1041-1051. DOI: 10.1093/jxb/erp374 (acccessed 4/27/2024).
(16) Trovato, M.; Funck, D.; Forlani, G.; Okumoto, S.; Amir, R. Editorial: Amino Acids in Plants: Regulation and Functions in Development and Stress Defense. *Frontiers in Plant Science* **2021**, *12*, Editorial. DOI: 10.3389/fpls.2021.772810.
(17) Lane, A. N.; Fan, T. W. M.; Xie, Z.; Moseley, H. N. B.; Higashi, R. M. Isotopomer analysis of lipid biosynthesis by high resolution mass spectrometry and NMR. *Anal. Chim. Acta* **2009**, *651* (2), 201-208. DOI: https://doi.org/10.1016/j.aca.2009.08.032. Metallo, C. M.; Gameiro, P. A.; Bell, E. L.; Mattaini, K. R.; Yang, J.; Hiller, K.; Jewell, C. M.; Johnson, Z. R.; Irvine, D. J.; Guarente, L.; et al. Reductive glutamine metabolism by IDH1 mediates lipogenesis under hypoxia. *Nature* **2012**, *481* (7381), 380-384. DOI: 10.1038/nature10602.

(18) Kertesz, V.; Van Berkel, G. J. Liquid Microjunction Surface Sampling Coupled with High-Pressure Liquid Chromatography−Electrospray Ionization-Mass Spectrometry for Analysis of Drugs and Metabolites in Whole-Body Thin Tissue Sections. *Anal. Chem.* **2010**, *82* (14), 5917-5921. DOI: 10.1021/ac100954p.
(19) Perdian, D. C.; Lee, Y. J. Imaging MS Methodology for More Chemical Information in Less Data Acquisition Time Utilizing a Hybrid Linear Ion Trap-Orbitrap Mass Spectrometer. *Anal. Chem.* **2010**, *82* (22), 9393-9400. DOI: 10.1021/ac102017q.
(20) Spraggins, J. M.; Djambazova, K. V.; Rivera, E. S.; Migas, L. G.; Neumann, E. K.; Fuetterer, A.; Suetering, J.; Goedecke, N.; Ly, A.; Van de Plas, R.; et al. High-Performance Molecular Imaging with MALDI Trapped Ion-Mobility Time-of-Flight (timsTOF) Mass Spectrometry. *Anal. Chem.* **2019**, *91* (22), 14552-14560. DOI: 10.1021/acs.analchem.9b03612.
(21) Unsihuay, D.; Mesa Sanchez, D.; Laskin, J. Quantitative Mass Spectrometry Imaging of Biological Systems. *Annu. Rev. Phys. Chem.* **2021**, *72* (1), 307-329. DOI: 10.1146/annurev-physchem-061020-053416 (acccessed 2023/01/06).
(22) Chumbley, C. W.; Reyzer, M. L.; Allen, J. L.; Marriner, G. A.; Via, L. E.; Barry, C. E., III; Caprioli, R. M. Absolute Quantitative MALDI Imaging Mass Spectrometry: A Case of Rifampicin in Liver Tissues. *Anal. Chem.* **2016**, *88* (4), 2392-2398. DOI: 10.1021/acs.analchem.5b04409.
(23) Wang, L.; Xing, X.; Zeng, X.; Jackson, S. R.; TeSlaa, T.; Al-Dalahmah, O.; Samarah, L. Z.; Goodwin, K.; Yang, L.; McReynolds, M. R.; et al. Spatially resolved isotope tracing reveals tissue metabolic activity. *Nat. Methods* **2022**, *19* (2), 223-230. DOI: 10.1038/s41592-021-01378-y.
(24) Palmer, A.; Phapale, P.; Chernyavsky, I.; Lavigne, R.; Fay, D.; Tarasov, A.; Kovalev, V.; Fuchser, J.; Nikolenko, S.; Pineau, C.; et al. FDR-controlled metabolite annotation for high-resolution imaging mass spectrometry. *Nat. Methods* **2017**, *14* (1), 57-60. DOI: 10.1038/nmeth.4072.

Table of Content Graphic